Atmospheric Research 315 (2025) 107934

Contents lists available at ScienceDirect

Atmospheric Research

journal homepage: www.elsevier.com/locate/atmosres

Characteristics of local recirculation affecting summer ozone in coastal areas of the Korean Peninsula

Jung-Woo Yoo [a], Soon-Hwan Lee [a,b,*]

[a] Institute of Environmental Studies, Pusan National University, Busan 46241, Republic of Korea
[b] Department of Earth Science Education, Pusan National University, Busan 46241, Republic of Korea

ARTICLE INFO

Keywords:
Ozone
Local circulation
Stagnation
Recirculation
Sea breeze

ABSTRACT

This study investigates the influence of local circulations, specifically stagnation and recirculation, on high ozone concentration events in Seoul during the summer (May–August) from 2016 to 2021. Local circulations were classified into Stagnation, Recirculation, and Ventilation types using the recirculation factor (RF), calculated as the ratio of net displacement distance (*L*) to actual displacement distance (*S*) based on wind observation data. Stagnation was the most frequently observed type, characterized by the highest daily maximum ozone concentrations and meteorological conditions unfavorable for dispersion, such as weak winds. During stagnation periods, limited air flow resulted in the accumulation of ozone within the urban area, with horizontal transport (HTRANS process) identified as a significant contributor to increased ozone concentrations near the surface. Additionally, nighttime ozone concentrations decreased due to active NO titration, accompanied by an increase in NO_2. In contrast, recirculation periods were marked by the presence of elevated ozone concentrations (~0.07 ppm) at altitudes above 500 m during the early morning. This residual ozone, transported offshore by nighttime land breezes, was brought back inland by daytime sea breezes and subsequently transported downward to the surface through vertical transport (VTRANS process), contributing significantly to surface ozone levels. The differences in ozone formation mechanisms between stagnation and recirculation highlight the role of limited dispersion in stagnation and the combined effects of sea breeze and vertical transport in recirculation. These findings emphasize the importance of understanding local circulation patterns, particularly the interaction between land and sea breezes, in predicting and managing high ozone events during the summer. The study underscores the need for long-term climatological research on local circulations and their impact on urban air quality to inform effective air quality management strategies.

1. Introduction

Surface ozone is recognized as a critical air quality issue worldwide. It is a major air pollutant with severe impacts on human health and the environment. Exposure to ozone can lead to various health issues, including respiratory and cardiovascular diseases. The risks are especially grave for vulnerable populations such as children, the elderly, and individuals with pre-existing respiratory conditions such as asthma (Silva et al., 2013; Day et al., 2017; Mirowsky et al., 2017). Zhang et al. (2019) showed that a 10 ppb increase in ozone concentration in China correlates with approximately 1 % rise in cardiovascular disease mortality. Additionally, ozone adversely impacts photosynthesis in plants, which reduces crop yield and quality (Hollaway et al., 2012; Grulke and Heath, 2020). Therefore, effectively managing surface ozone levels is crucial for air quality management. Ozone is not emitted directly from sources; rather, it is a secondary pollutant formed via photochemical reactions between nitrogen oxides (NOx) and volatile organic compounds (VOCs) in the presence of solar radiation. NO_2 is formed by sunlight to produce NO and an oxygen atom in Eq. (1), which then combines with molecular oxygen to form ozone in Eq. (2). Ozone (O_3) reacts with NO, regenerating NO_2 and producing oxygen in Eq. (3).

$$NO_2 + h\nu \rightarrow NO + O \quad (1)$$

$$O + O_2 \rightarrow O_3 \quad (2)$$

$$O_3 + NO \rightarrow NO_2 + O_2 \quad (3)$$

Surface ozone is a secondary pollutant formed through

* Corresponding author at: Department of Earth Science Education, Pusan National University, Busan 46241, Republic of Korea.
E-mail address: withshlee@pusan.ac.kr (S.-H. Lee).

https://doi.org/10.1016/j.atmosres.2025.107934
Received 28 August 2024; Received in revised form 3 January 2025; Accepted 18 January 2025
Available online 19 January 2025

photochemical reactions involving its precursors, nitrogen oxides (NOx) and volatile organic compounds (VOCs). Major sources of these precursors include vehicle emissions and industrial activities. Despite efforts in South Korea to reduce NOx and VOC emissions to control ozone levels, surface ozone concentrations have continued to rise (Yeo and Kim, 2021; Colombi et al., 2023). This indicates that effective ozone mitigation requires not only emission reductions but also a comprehensive understanding of the various factors influencing ozone formation and distribution. As a secondary pollutant, ozone exhibits significant spatial and temporal variability due to its dependence on precursor emissions. High ozone concentrations are influenced by various factors, including anthropogenic emissions of precursors such as NOx and VOCs (Seo et al., 2014; Kim et al., 2021), long-range transport of pollutants (Cuesta et al., 2018), changes in ozone chemical regimes (Sillman, 1999), and stratospheric ozone intrusion (Shin et al., 2020). During the period from 2015 to 2019, NOx emissions in Seoul decreased by approximately 30 % (Seo et al., 2021). However, the Seoul Metropolitan Area (SMA), home to about 50 % of South Korea's population, continued to experience frequent exceedances of ozone concentrations above 0.09 ppm (Miyazaki et al., 2019). This highlights the persistent severity of high ozone levels in the SMA despite precursor emission reductions.

Meteorological conditions, such as solar radiation, temperature, cloud cover, relative humidity, and wind, also play a critical role in ozone formation. Particularly, O_3 distribution is significantly influenced by these meteorological factors, which are closely related to regional transport and chemical formation (An et al., 2015; Li et al., 2018). Moreover, atmospheric circulation patterns, including synoptic and mesoscale circulations, significantly influence the transport and distribution of ozone (Dueñas et al., 2002; Martins et al., 2012; Han et al., 2020). For example, in the Pearl River Delta region of China, strong downdrafts associated with typhoons have been observed to vertically transport residual ozone from the upper layers to the surface, leading to elevated ozone levels (Liu et al., 2023). Additionally, the increased frequency of high-pressure systems over Eurasia and North America, driven by climate change, has contributed to atmospheric stagnation and exacerbated summer ozone episodes. The influence of cold fronts and lee troughs, which are accompanied by strong winds and enhance horizontal transport of pollutants from upwind regions, further impacts downwind air quality and surface ozone levels (Yoo et al., 2022; Yoo et al., 2024a).

In urban areas, mesoscale circulations, such as land-sea breezes and mountain-valley winds, are particularly important in determining the diurnal variation and spatial distribution of surface ozone. These circulations drive the transport and accumulation of ozone and its precursors during the daytime and facilitate their redistribution at night (Hu et al., 2018). For instance, Zhang et al. (2024) demonstrated that mountain-valley winds in mountainous regions contribute to a 14.8 % increase in surface ozone concentrations by transporting ozone and its precursors. In coastal areas like the Houston–Galveston region, sea breezes during the summer are reported as a major factor in elevated ozone levels (Caicedo et al., 2019; Li et al., 2020). Strong sea breezes can mix upper atmospheric pollutants down to the surface, further increasing ozone concentrations (He et al., 2022). Additionally, ozone's low solubility allows it to recirculate inland via sea breezes the following day, with the alternating action of land and sea breezes resulting in pollutant recirculation and accumulation (Caicedo et al., 2019). In New York, weak synoptic winds enhance land-sea breeze circulations, mixing newly emitted pollutants with recirculated ones, which degrades air quality and increases surface ozone concentrations (Nauth et al., 2023; Wu et al., 2010; Martins et al., 2012; Loughner et al., 2014). Similarly, Monteiro et al. (2012) identified that ozone recirculation driven by mountain breezes and sea-breeze circulations leads to elevated ozone levels in mountainous regions.

Atmospheric stagnation, characterized by weak winds and stable meteorological conditions, also plays a critical role in high ozone episodes. Stagnation typically occurs within high-pressure systems, where horizontal dispersion and vertical mixing are suppressed, resulting in pollutant accumulation (Jacob and Winner, 2009; Garrido-Perez et al., 2018; Yoo et al., 2024b). This effect is particularly pronounced in urban areas with high emissions. For example, the Western Pacific Subtropical High has been shown to create inversion layers and weak winds in China, limiting pollutant dispersion and causing ozone accumulation near the surface (Liu et al., 2023). Additionally, the increased frequency of dry tropical synoptic patterns (hot and dry conditions) has been closely linked to enhanced ozone formation (Kim et al., 2021).

Understanding the mechanisms behind high ozone concentrations under complex meteorological conditions is essential for effective ozone pollution management. Local circulations, such as land-sea breezes, are particularly important in shaping the diurnal variation of ozone levels in urban areas. This study focuses on the role of local circulations in high ozone formation by classifying summer winds in Seoul into the Recirculation, Stagnation, and Ventilation types. Through observational data and numerical simulations, the study quantitatively assesses the contributions of these local circulation types to surface ozone levels, providing valuable insights into the mechanisms underlying urban ozone pollution in the SMA.

2. Methods

2.1. Recirculation factor

In this study, we applied the L and S indices and the recirculation index proposed by Allwine and Whiteman (1994) to classify local winds. The method for calculating the recirculation index is as follows:

$$L = \sqrt{\left(\sum_{j=i}^{i-\tau+1} T \times u_j\right)^2 + \left(\sum_{j=i}^{i-\tau+1} T \times v_j\right)^2}$$

$$S = \sum_{j=i}^{i-\tau+1} \sqrt{\left(T \times u_j\right)^2 + \left(T \times v_j\right)^2}$$

$$\mathrm{RF} = 1 - \frac{L}{S}$$

τ represents 24, T is the time interval (24 h), and u_j and v_j represent the east–west and north–south wind components, respectively. L represents the net displacement distance of the air parcel over 24 h, while S represents the actual distance traveled. The recirculation factor (RF) is determined by the ratio of L to S; a value closer to 1 indicates a shorter L, suggesting a higher likelihood of air recirculation. Conversely, a value closer to 0 indicates that the air has moved in a straight line over a longer distance, suggesting a lower likelihood of recirculation and more favorable ventilation conditions. A low RF value indicates a low probability of horizontal recirculation, but it does not rule out the possibility of vertical recirculation (Levy et al., 2008). The assessment of horizontal recirculation likelihood enables a straightforward explanation of pollutant transport conditions (Russo et al., 2016). Previous studies, using the calculated RF, have confirmed that ozone concentration increases during recirculation events (Levy et al., 2008; Lee et al., 2015). In this study, L, S, and RF were calculated using ground-based observational data, and thus are considered as indicators of regional-scale wind fields near the observation site. Nevertheless, this approach provides valuable insights for investigating the climatological characteristics of regional-scale airflows and pollutant transport in various areas in an intuitive manner (Levy et al., 2008; Russo et al., 2016).

2.2. Classification of local circulation pattern

Allwine and Whiteman (1994) proposed critical values using the S and RF indices to classify airflows in the Grand Canyon region of the

United States into categories of recirculation, stagnation, and ventilation. Although this method considers only the horizontal movement of the atmosphere, it has been proven effective for analyzing pollutant dispersion (Wang et al., 2022).

$$\begin{cases} S \leq 170\text{km}\ (\text{WS} \sim 2\text{ms}^{-1}) : \text{site is prone to stagnation} \\ \text{RF} \geq 0.4 : \text{stie is prone to recirculation} \\ S \geq 250\text{km and RF} \leq 0.2 : \text{site is prone to ventilation} \end{cases}$$

Where WS is the average daily wind speed.

In South Korea, days with an average wind speed of less than 2 m s^{-1} are classified as stagnation, similar to the critical values proposed by Allwine and Whiteman (1994). Meanwhile, Levy et al. (2010) proposed a critical value based on the average recirculation index and standard deviation, using data from multiple observation sites. Additionally, Russo et al. (2016) suggested empirical critical values for different scales of atmospheric circulation by employing K-means clustering and recirculation index calculation. However, these critical values were developed based on wind data observed in specific regions, which may not be suitable for application in other areas. Therefore, Russo et al. (2018) proposed critical values that take into account both wind fields and regional characteristics.

$$\begin{cases} S \leq S_{avg} : \text{site is prone to stagnation} \\ \text{RF} \geq \text{RF}_{avg} : \text{stie is prone to recirculation} \\ S \geq S_{cv} \text{ and RF} \leq \text{RF}_{cv} : \text{site is prone to ventilation} \\ S_{cv} = \text{P75(S)}, \text{RF}_{cv} = \text{P25(RF)} \end{cases}$$

where S_{avg} and RF_{avg} are the average values of *S* and RF, S_{cv} and RF_{cv} are the critical values of *S* and RF, and P75 and P25 represent the 75th and 25th percentiles, respectively.

In this study, we referenced previous research to calculate the daily *L*, *S*, and RF indices for Seoul using hourly wind speed data from May to August during the 2016–2021 period. Based on these calculations, we classified the local circulation in Seoul into the Stagnation, Recirculation, and Ventilation types as outlined below:

$$\begin{cases} \text{WS} < 2\text{ms}^{-1} : \text{site is prone to stagnation} \\ \text{RF} \geq \text{RF}_{avg} : \text{stie is prone to recirculation} \\ S \geq S_{cv} \text{ and RF} \leq \text{RF}_{cv} : \text{site is prone to ventilation} \\ S_{cv} = \text{P75(S)}, \text{RF}_{cv} = \text{P25(RF)} \end{cases}$$

2.3. Observational data

To classify the local circulation in Seoul, we used meteorological observations and ozone and NO_2 concentration measurements from May to August (total of 738 days) during 2016–2021, excluding precipitation days. The meteorological data for Seoul were obtained from the Korea Meteorological Administration (KMA)'s Automated Synoptic Observing System (ASOS) stations, which provided hourly 10-m wind speed and direction, as well as relative humidity data (Yellow star in Fig. 1). Additionally, ozone concentration measurements were drawn from 25 Air Quality Monitoring Stations (AQMS) across Seoul, managed by the National Institute of Environmental Research (Red circles in Fig. 1). Additionally, to evaluate the performance of the WRF meteorological model results, hourly 2-m temperature (T2) and 10-m wind speed (WS10) data observed at 39 ASOS stations within the d03 domain were used (Yellow star and black triangles in Fig. 1). For the evaluation of the CMAQ air quality model results, ozone concentration data from 191 AQMS stations were utilized (Red and blue circles in Fig. 1).

2.4. Meteorological and air quality models

In this study, meteorological and air quality numerical simulations were conducted to investigate the transport of ozone under local circulation conditions. The Weather Research and Forecasting (WRF, version 3.9.1.1) model (Skamarock et al., 2008) is the meteorological model applied in this study. The Community Multiscale Air Quality Modeling System (CMAQ, version 5.2) model (Byun and Schere, 2006) is the air quality model used. Three domains were set up in total, with the innermost domain, d03, centered over Seoul and configured with a horizontal resolution of 3 km (Fig. 1). Initial and boundary conditions for the WRF model were provided by the Final Operational Global Analysis (FNL) reanalysis data from the National Centers for Environmental Prediction (NCEP), with a horizontal resolution of 0.25° x 0.25° and a temporal resolution of 6 h. Detailed physics options are listed in Table S1. In this study, grid nudging was applied to the U and V wind components, potential temperature, and water vapor mixing ratio in the d01 and d02 domains to more accurately simulate local circulations.

The anthropogenic emissions data for the CMAQ model were sourced from The Emissions Database for Global Atmospheric Research (EDGARv6.1; https://edgar.jrc.ec.europa.eu/dataset_ap61, last accessed: June 2023) for international data and the Clean Air Policy Support System (CAPSS) for domestic data. The biogenic emissions were calculated using the Model of Emissions of Gases and Aerosols from Nature (MEGAN version 2.1). The chemical mechanism used was the Carbon Bond 05 (CB05) mechanism with updated toluene chemistry (CB05tucl),

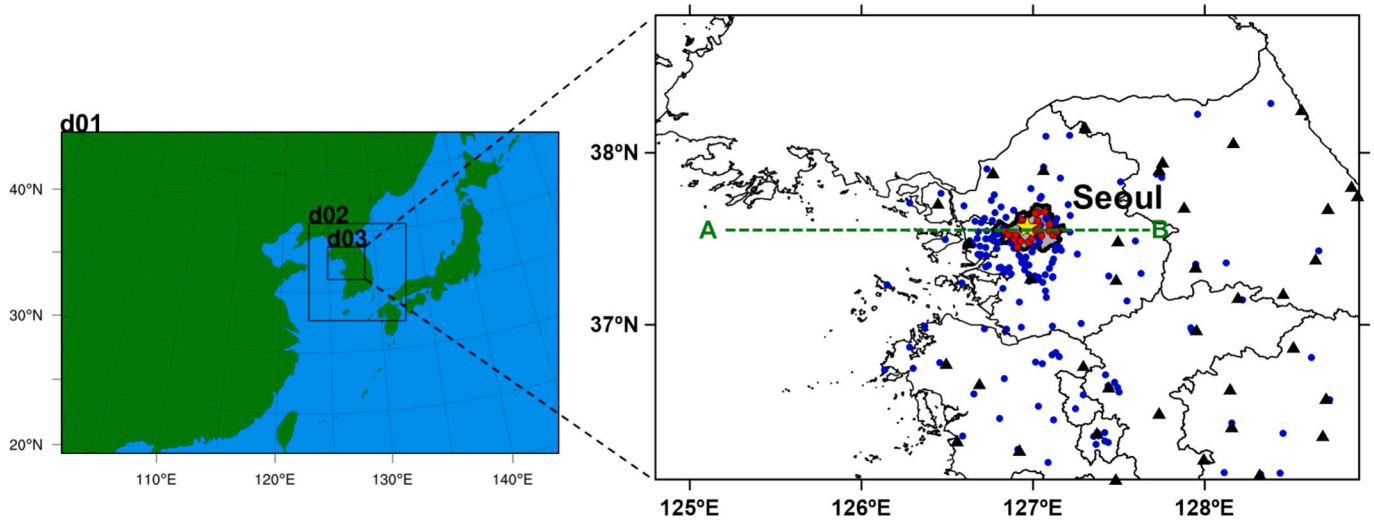

Fig. 1. The modeling domain for simulations. Black triangles and blue circles represent the Automated Synoptic Observing System (ASOS) and Air Quality Monitoring Station (AQMS) sites, respectively. Yellow star and red circles represent the meteorological observation and O_3 measurement sites in Seoul, respectively. (For interpretation of the references to colour in this figure legend, the reader is referred to the web version of this article.)

and the AERO6 aerosol module was employed for the gas-phase and aqueous-phase chemistry mechanisms.

The Integrated Process Rate (IPR) method (Gipson, 1999) of the CMAQ model was used to investigate the contributions of processes to surface ozone concentration in Seoul. IPR is a Process Analysis (PA) method that calculates the physical and chemical processes affecting pollutant concentrations in each grid cell, enabling a quantitative comparison of their contributions. This process includes horizontal and vertical advection (HADV and ZADV) and diffusion (HDIF and VDIF), emissions (EMIS), gas-phase chemistry (CHEM), aerosols (AERO), deposition (DDEP), and cloud processes (CLDS). In this study, horizontal advection and diffusion were combined and calculated as horizontal transport (HTRANS), while vertical advection and diffusion were combined and calculated as vertical transport (VTRANS) to analyze their contributions to ozone concentration.

3. Results

3.1. Classification results of local circulation

The local circulation in Seoul were classified into the Stagnation, Recirculation, and Ventilation types using the hourly wind speed observations from May to August, covering the period from 2016 to 2021. Days classified as the Stagnation type accounted for 251 days (34 %), making it the most dominant type of local circulation observed in Seoul. Days classified as the Recirculation type accounted for 113 days (16 %), while those classified as the Ventilation type accounted for 38 days (5 %).

Fig. 2 presents the box plot of daily maximum ozone levels for classified local circulation types. A comparison of ozone concentration distributions for each type shows that the Stagnation type exhibits the highest variability, with a mean value of 0.072 ppm. Additionally, the daily average wind speed for this type is 1.65 ms^{-1}, indicating very weak winds that can lead to ozone accumulation and elevated concentrations due to atmospheric stagnation. The Recirculation type demonstrates relatively uniform ozone concentrations, with a mean value of 0.066 ppm, and a daily average wind speed of 2.34 ms^{-1}. For the Ventilation type, although outliers are observed, their frequency is very low, and the mean value (0.067 ppm) is comparable to that of the Recirculation type. Moreover, the daily average wind speed for the Ventilation type is 2.43 ms^{-1}, significantly stronger than other types, suggesting that pollutants, including ozone, are dispersed and diluted more effectively, potentially lowering concentrations.

Fig. 3 illustrates the diurnal variations of ozone and NO_2 concentrations for different local circulation types. A consistent pattern is observed across all types, with higher ozone concentrations during the daytime due to increased photochemical activity driven by rising temperatures. The highest daily ozone concentration was recorded under the Stagnation type at 17:00 LST, reaching 0.067 ppm, while the Recirculation and Ventilation types recorded 0.063 ppm and 0.058 ppm, respectively, at 16:00 LST. Interestingly, the Stagnation type, which exhibited the highest peak ozone concentration, also had the lowest nighttime ozone concentration. This is due to significant anthropogenic NOx emissions in metropolitan areas, which lead to the NO titration effect at night, causing rapid ozone depletion (Ghim and Chang, 2000; Hu et al., 2012). During stagnation, weak winds (Fig. S1) prevent the dispersion of locally emitted pollutants, leading to the accumulation of NOx within the urban environment. This results in reduced ozone levels through chemical loss processes, particularly during the early evening when local emissions remain active. The corresponding increase in NO_2 during these periods further supports the occurrence of NO titration (Fig. 2). In contrast, the Ventilation type, characterized by the highest average daily wind speed, exhibited the lowest peak ozone concentration and the highest trough concentration. This suggests that stronger winds in the Ventilation type enhance the dispersion and dilution of pollutants, preventing the buildup of ozone and NOx.

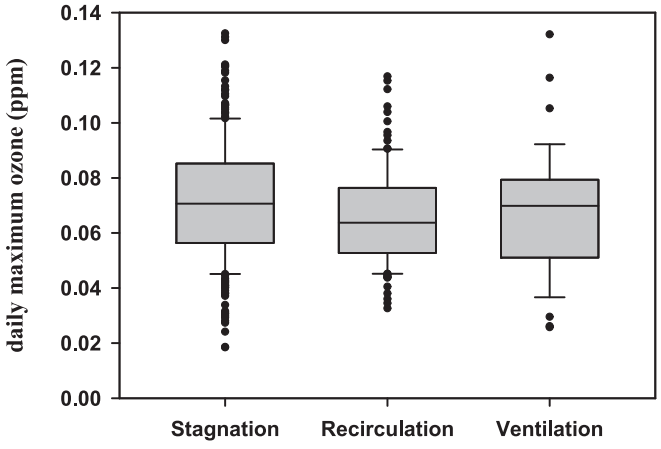

Fig. 2. Box plots of daily maximum ozone concentration by local circulation type.

Fig. 4 presents the average ozone mixing ratio at 09:00 LST at 925 hPa, derived from the ERA5 reanalysis data, for days classified as the Stagnation, Recirculation, and Ventilation types. The ozone mixing ratio included in the ERA5 reanalysis data (horizontal resolution of 0.25° x 0.25°) is linearly estimated considering temperature, stratospheric chlorine concentration, altitude, and season (Cariolle and Teyssèdre, 2007). As shown in Fig. 3, the ozone mixing ratio at 09:00 LST is higher for the Recirculation type compared to the Stagnation type. Notably, regions west of Seoul, including coastal and ocean regions, exhibit relatively higher ozone mixing ratios compared to the Stagnation type. This suggests that the interaction between sea breeze and land breeze in the Recirculation type may serve as a critical factor contributing to the increase in daytime ozone concentrations in Seoul.

3.2. Episode description

To investigate the impact of atmospheric stagnation and air recirculation on ozone concentration in Seoul, we selected days with high ozone levels for each type of stagnation and recirculation. July 5, 2019, was classified as a stagnation day in Seoul due to its low average daily wind speed of 1.5 ms^{-1}. On this day, the daily peak ozone concentration was notably high, reaching 0.121 ppm. The weather on this day was clear under the influence of high pressure over the East Sea (Fig. S2), and the maximum temperature in Seoul reached 35.0 °C. This high temperature acted as a key factor in promoting photochemical reactions, leading to active ozone formation. Consequently, the daily peak ozone concentration on this day was exceptionally high, recorded at 0.121 ppm. Observational data analysis reveals that from 00:00 to 14:00 LST, a range of wind directions, including weak north winds with speeds of 1.5 ms^{-1}, as well as east and west winds, were observed. Although westerly winds were present during the day, the characteristics of a sea breeze, such as increased relative humidity, were not evident (see Fig. 5 (a)). To examine air mass movement on the case study day, the FLEXPART-WRFV3.3 model (Brioude et al., 2013), developed by the Norwegian Institute for Air Research, and was utilized. The simulation involved releasing 1000 particles from 0 to 20-m above ground level in Seoul at 18:00 LST on the case-study day and performing a 24-h backward trajectory analysis, with results presented at 6-h intervals (see Fig. 6). On the stagnation date, particles released in Seoul were observed to remain in the surrounding area of the city until 18 h later, indicating extremely short particle travel distance because of atmospheric stagnation. The recirculation date was selected as May 3, 2017, when the average daily wind speed in Seoul was 2.0 ms^{-1} and the daily maximum ozone concentration was 0.115 ppm. Additionally, the RF was 0.51, indicating a high probability of a recirculation event. On this day, Seoul was under the influence of high pressure over the East Sea, with widely spaced

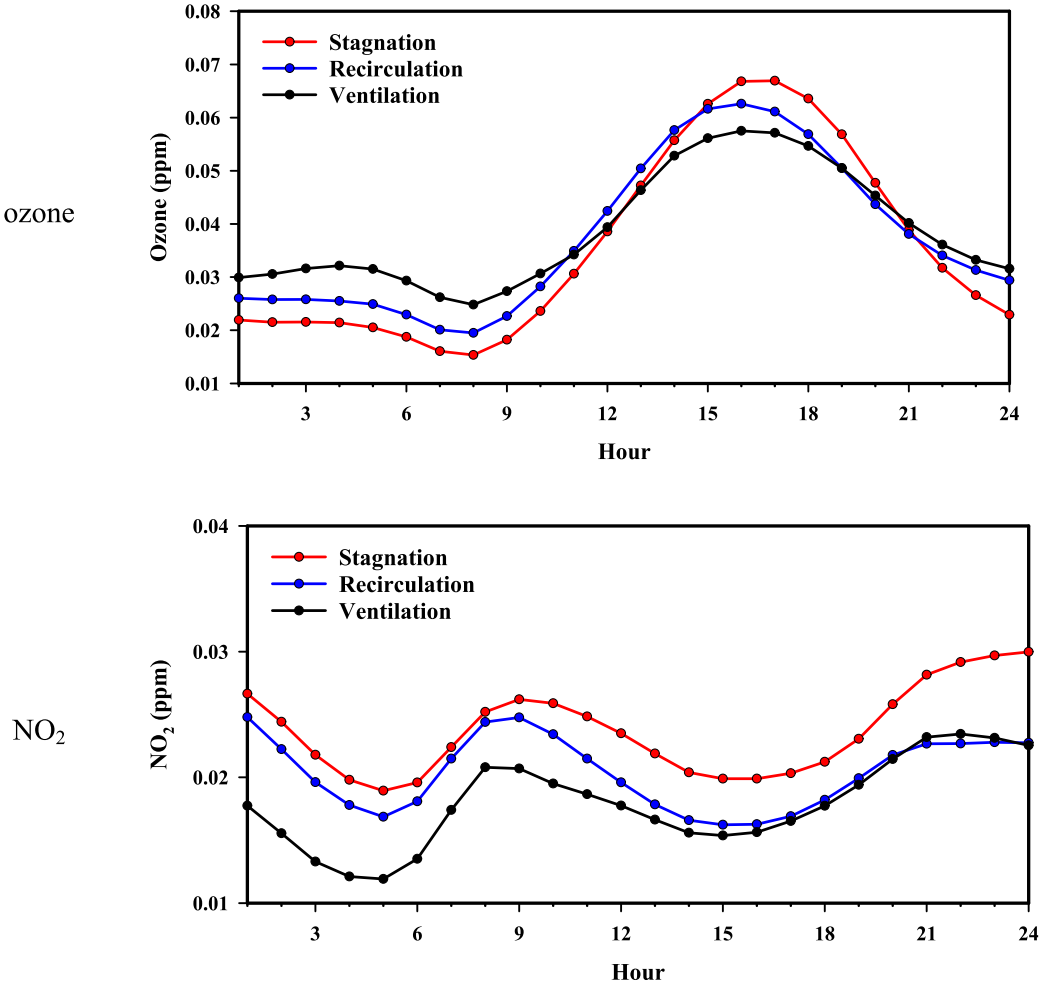

Fig. 3. Diurnal variation of ozone and NO_2 concentrations by local circulation type.

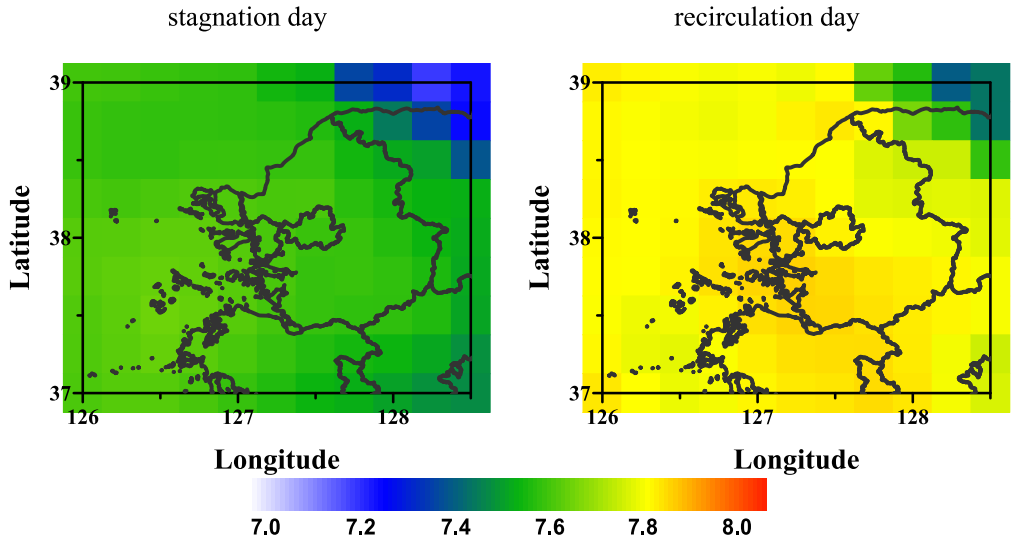

Fig. 4. The horizontal distribution of ozone mixing ratio ($kg \cdot kg^{-1}$) from ERA5 reanalysis data at 950 hPa.

isobars reducing the impact of synoptic-scale winds (Fig. S2). These conditions were favorable for the development of mesoscale winds, such as land-sea breezes. Furthermore, the maximum temperature in Seoul was recorded at 30.2 °C, with an average wind speed of 2.0 ms^{-1}, contributing to a high peak ozone concentration of 0.115 ppm. Unlike on the stagnation day (Fig. 5 (a)), the recirculation day exhibited less variation in wind direction, with easterly (land breeze) and westerly (sea breeze) winds persisting for relatively extended periods (Fig. 5 (b)). In the morning, southerly and easterly winds were observed. By 14:00 LST, the increase in wind speed and relative humidity, along with the

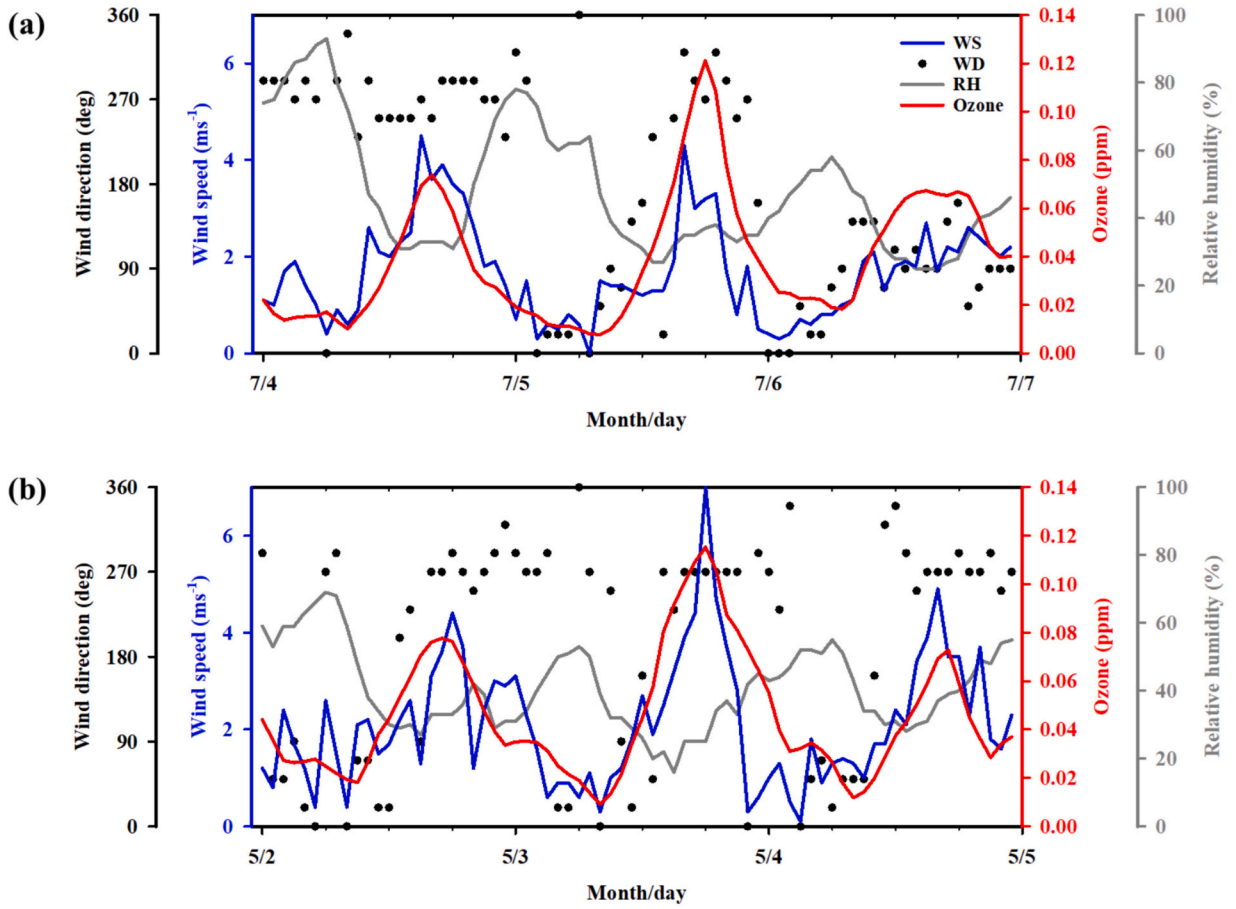

Fig. 5. Temporal variation of ozone concentration, wind speed and direction, and relative humidity on (a) stagnation day and (b) recirculation day in Seoul.

presence of westerly winds, suggested that these changes were likely due to the arrival of a sea breeze. Additionally, an increase in ozone concentration of 0.023 ppm was observed compared with that at 13:00 LST. In the 24-h backward trajectory analysis, particles that were moving southwest at 12:00 LST on May 3, 2017, were found to have moved back toward Seoul by 00:00 LST on the same day, 18 h earlier.

In other words, particles that were transported to sea due to nighttime land breezes (easterly and northeasterly winds) were brought back to Seoul by westerly winds during the recirculation day, indicating the occurrence of a recirculation phenomenon. Therefore, this case is suitable for studying the impact of air recirculation on ozone concentration in Seoul.

3.3. Model evaluation

To evaluate the performance of the WRF model, we used 2-m temperature (T2) and 10-m wind speed (WS10) from 39 ASOS sites within Domain 3. The statistical metrics for performance evaluation included the Mean Bias (MB), Index of Agreement (IOA), and Correlation Coefficient (R). Values of R and IOA closer to 1 and MB closer to 0 indicate greater similarity between the model results and the observations.

Statistical evaluation was performed over a total of five days, including the case day, with a spin-up time of five days excluded. Both on the stagnation and recirculation days, the WRF model results for T2 showed a tendency to slightly underestimate compared to the observations. However, the Index of Agreement (IOA) was above 0.9, indicating that the model effectively simulates the temperature trends important for photochemical reactions (Table 1). Regarding WS10, although the WRF model slightly overestimated the observations, it provided satisfactory results in simulating daily variability. The evaluation of the WRF model's performance revealed that it generally satisfied the criteria proposed by Emery et al. (2001) for T2 (Mean Bias $\leq \pm 0.5$ °C, IOA $\geq$ 0.7) and WS10 (Mean Bias $\leq \pm 0.5$ ms^{-1}, IOA $\geq$ 0.6).

Additionally, the performance of the CMAQ model was evaluated by comparing the ozone concentration measured at 190 AQMS sites with the results from the model. Generally, the simulated ozone concentrations were in good agreement with the measured data. The CMAQ model tended to slightly overestimate ozone concentration on the stagnation day and slightly underestimate on the recirculation day. However, the IOA (R) values were 0.81 (0.70) and 0.76 (0.60), respectively, indicating that the model effectively captured the overall trends. Therefore, based on the performance evaluation of the meteorological and air quality models in this study, it was determined that they are suitable for analyzing local circulation and the resulting variability in ozone concentration.

3.4. Horizontal distribution of ozone

Generally, ozone levels increase during the daytime due to active photochemical reactions and decrease at night. At the surface, the horizontal distribution of ozone showed no significant differences between stagnation and recirculation days, suggesting that the mechanisms driving high ozone concentrations may appear similar at this level (Fig. S3). However, previous analysis of the ozone mixing ratio at 950 hPa at 09:00 LST revealed that ozone concentrations were higher over the ocean than over land on recirculation days (Fig. 4). Based on this observation, the horizontal distribution of ozone at layer 6 (approximately 560 m altitude) was analyzed and is presented in Fig. 7. The

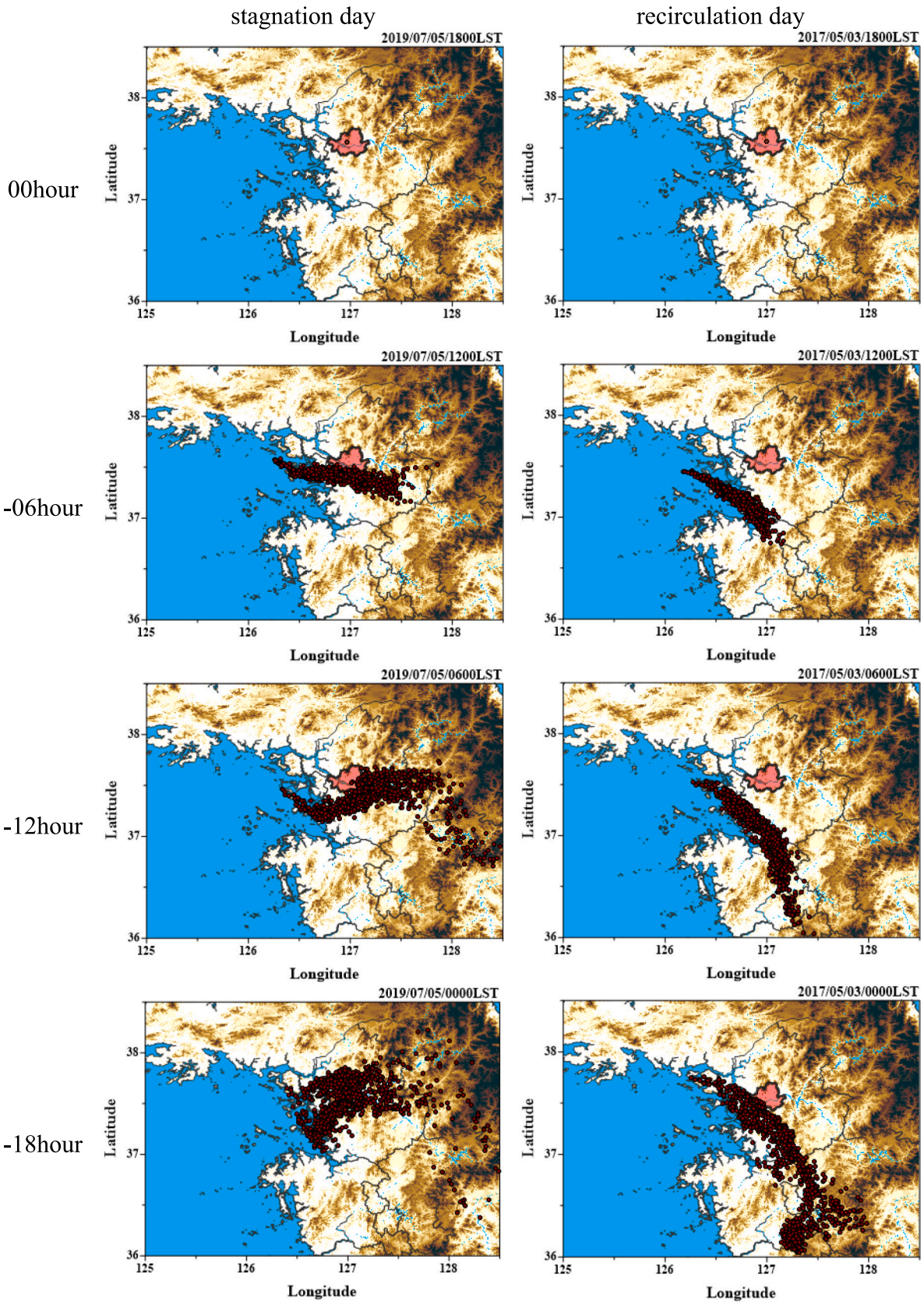

Fig. 6. 24-h back-trajectories calculated every 6-h for stagnation and recirculation days.

Table 1
Statistical metrics results of simulated temperature at 2 m (T2), wind speed at 10 m, and ozone concentration.

		Obs. mean	Model mean	MB	IOA	R
stagnation day	T2	24.17 °C	23.97 °C	−0.20 °C	0.96	0.93
	WS10	1.48 ms^{-1}	1.94 ms^{-1}	0.46 ms^{-1}	0.76	0.62
	ozone	0.042 ppm	0.045 ppm	0.004 ppm	0.81	0.70
recirculation day	T2	18.50 °C	17.81 °C	−0.69 °C	0.94	0.91
	WS10	1.72 ms^{-1}	2.27 ms^{-1}	0.55 ms^{-1}	0.79	0.68
	ozone	0.051 ppm	0.048 ppm	−0.003 ppm	0.76	0.60

results showed that, similar to the pattern observed at 950 hPa, ozone concentrations were higher over the ocean than over land at layer 6 on recirculation days. This suggests that residual ozone from the previous day over the sea could be transported inland by the sea breeze, contributing to the increase in ozone concentrations in Seoul. These findings highlight the potential role of residual ozone over the ocean in influencing ozone levels in urban areas such as Seoul through mesoscale transport mechanisms like sea breeze circulation.

3.5. Vertical distribution of ozone

Fig. 8 illustrates the temporal variations in vertical ozone concentration profiles averaged over Seoul for a stagnation day (July 5) and a recirculation day (May 3). On the stagnation day, July 5, surface ozone concentrations were low in the early morning, below 0.02 ppm. However, as solar radiation increased during the morning, photochemical reactions led to a rapid rise in ozone concentration. By the afternoon, high ozone concentrations (~0.1 ppm) extended up to ~1.5 km altitude due to the growth of the planetary boundary layer. The highest surface ozone concentration, 0.11 ppm, was recorded at 18:00 LST. In contrast, on the recirculation day, May 3, high ozone concentrations exceeding 0.1 ppm were observed from the surface to ~1.5 km altitude after 15:00 LST. Unlike the stagnation day, significant ozone concentrations (0.05–0.07 ppm) were detected at altitudes of 500 m to 1 km in the early morning. This residual ozone layer shows a pattern consistent with the ozone mixing ratio distribution at 950 hPa (Fig. 4), suggesting that ozone formed during the previous day persisted overnight in the atmosphere.

To investigate the origin of this residual ozone, the vertical cross-section of ozone concentration along the A–B line in Fig. 1 was analyzed (Fig. 9). At 00:00 LST on the recirculation day, ozone concentrations exceeding 0.07 ppm were detected above 500 m altitude. At 09:00 LST, residual ozone remained near 500 m altitude over the sea (near longitude 126.2°). This indicates that ozone formed the previous day remained in the atmosphere overnight. During the daytime, this residual ozone could be transported inland by sea breeze, contributing to elevated ozone concentrations in Seoul. At 17:00 LST, ozone concentrations above 1.5 km altitude near longitude 127.0° were observed, likely as a result of photochemical reactions that had been actively occurring under strong sunlight throughout the day. Additionally, a counterclockwise sea breeze circulation was observed in the upper

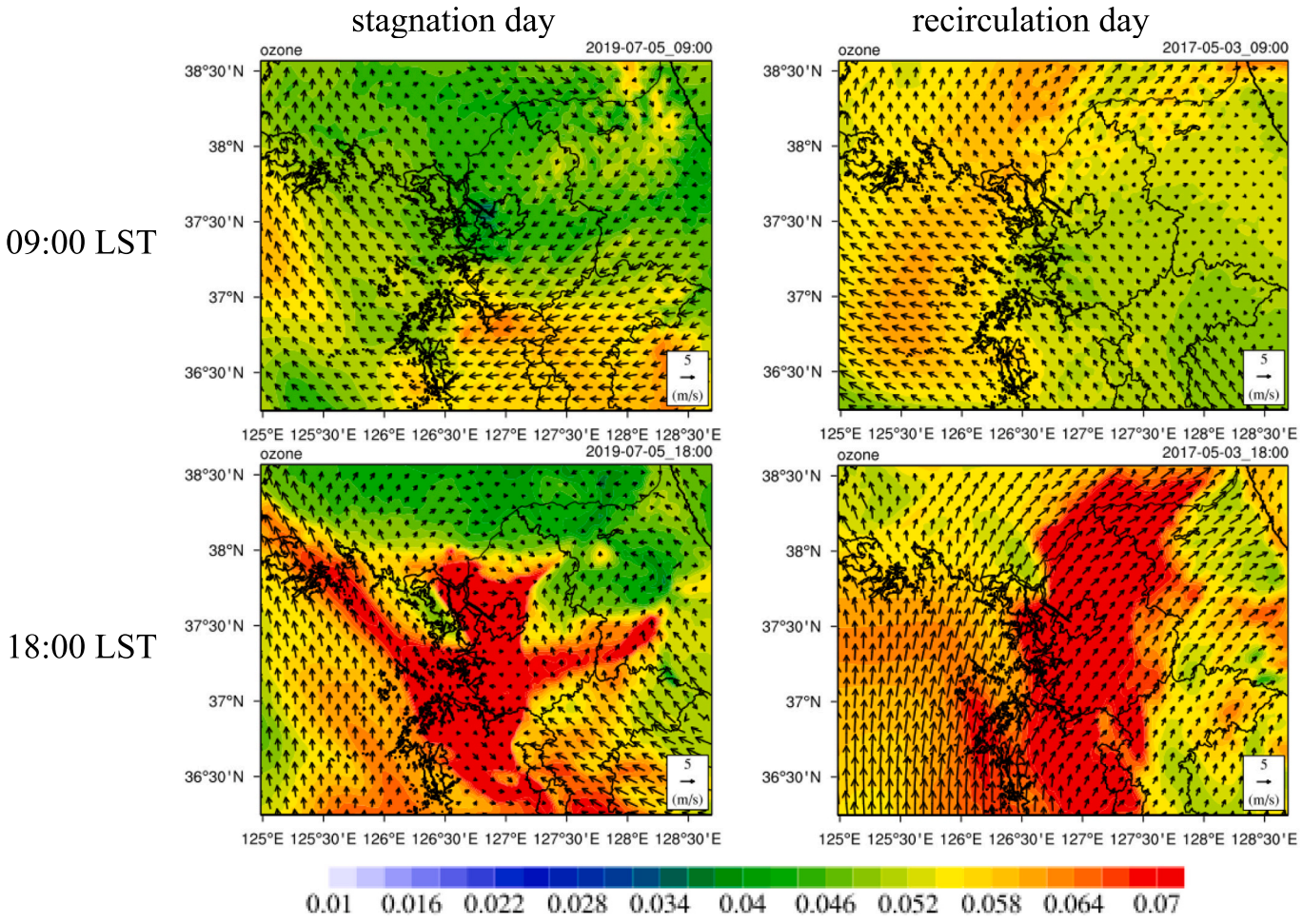

Fig. 7. The horizontal distribution of ozone at layer 6 (about 560-m) altitude, on stagnation and recirculation days.

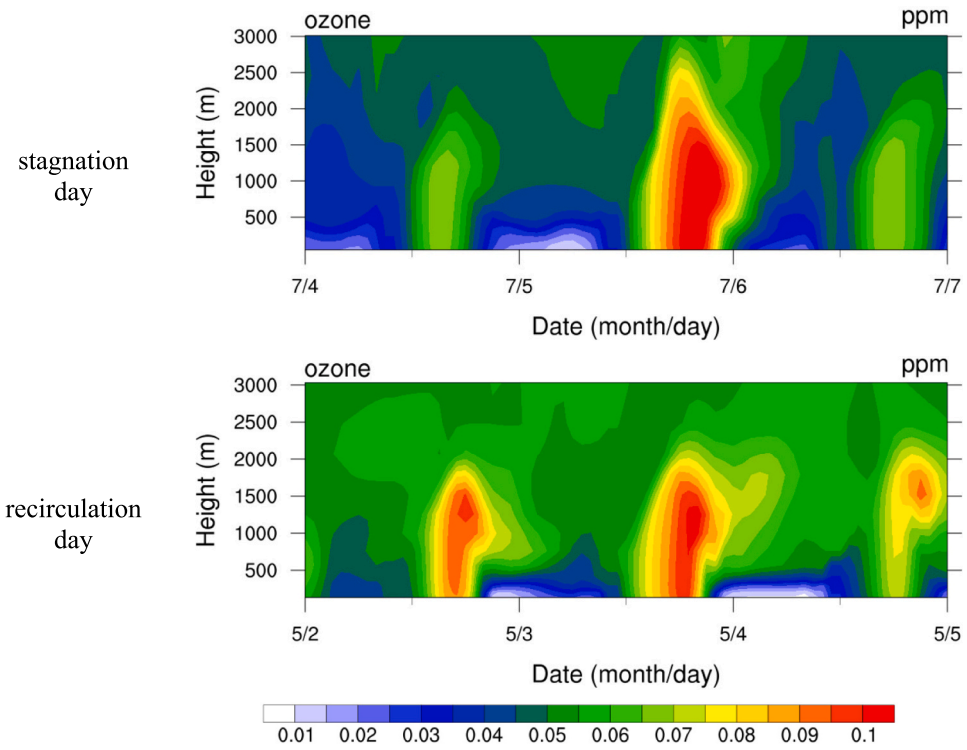

Fig. 8. Time series of time-height sections of ozone over Seoul.

layers over Seoul. This circulation, driven by thermal differences between the sea and land or rural and urban areas, represents secondary circulation (Abe and Yoshida, 1982; Freitas et al., 2007). In urban areas such as Seoul, the urban heat island effect can enhance the inland penetration of sea breezes and strengthen secondary circulation (Freitas et al., 2007). These secondary circulations enhance mixing between the upper and lower layers, encouraging the vertical transport of residual ozone from ~500 m altitude to the surface. Thus, photochemical ozone production during the daytime and vertical transport of residual ozone through secondary circulation are likely key mechanisms increasing ozone concentrations in Seoul on recirculation day. On the other hand, no significant residual ozone was observed over the sea during nighttime or early morning on stagnation day. This suggests that the conditions necessary for residual ozone to form over the sea on recirculation day are not present during stagnation day. The extremely weak air flow on stagnation day likely inhibits the transport of pollutants from urban areas to the sea via the nighttime land breeze, causing them to remain within the city. As a result, these pollutants accumulate within the urban area, further contributing to elevated local pollution levels. At night on stagnation day, the weak air flow leads to the accumulation of ozone within the city, creating conditions for an intensified NO titration effect due to elevated ozone levels. As a result, surface ozone concentrations are significantly reduced, falling below 0.04 ppm in Seoul. By 17:00 LST on stagnation day, ozone concentrations increased up to ~2 km altitude due to strong photochemical reactions under intense sunlight. However, due to atmospheric stagnation, the newly formed ozone is unlikely to disperse to surrounding areas and remains trapped within the city. Similar to recirculation day, secondary circulations were observed on stagnation days, facilitating the vertical mixing of ozone produced by photochemical reactions from the upper layers to the surface.

In summary, recirculation days are characterized by the transport of residual ozone from the sea to urban areas through sea breezes, significantly contributing to increased ozone levels in the city. In contrast, stagnation days are dominated by the accumulation of newly formed ozone within urban areas, primarily due to limited dispersion under weak atmospheric flow. These differences highlight the distinct mechanisms by which ozone concentrations are elevated on each type of day.

3.6. Contribution of processes affecting ozone

To investigate the processes contributing to surface ozone level increases in Seoul during stagnation and recirculation days, an analysis of ozone-affecting processes by vertical layers was conducted. The study focused on the average IPR results during the daytime hours (12:00–18:00 LST), when ozone concentrations were elevated. Specifically, the model's 12th layer (approximately 3 km altitude) was examined (Fig. 10). The IPR analysis quantified the contributions of horizontal transport (HTRANS) and vertical transport (VTRANS) processes to ozone concentrations. Positive values in the IPR results indicate that the respective processes (HTRANS or VTRANS) contributed to an increase in ozone concentration through ozone transport.

On stagnation day, horizontal transport (HTRANS) from the surface up to layer 6 (approximately 560 m) was identified as a significant contributor to surface ozone levels. This reflects ozone transported from upwind areas to Seoul via horizontal advection. However, weak air flow during stagnation limited advection and dispersion from Seoul to downwind areas, resulting in the local accumulation of ozone. Consequently, the HTRANS process contributed an average increase of 0.004 ppm in surface ozone concentrations during the daytime. Additionally, the vertical transport (VTRANS) process also played a significant role on stagnation day, contributing an average increase of 0.01 ppm to surface ozone concentrations. As described in Section 3.5, this vertical transport was driven by secondary circulations, which facilitated the downward mixing of ozone produced in the upper layers through photochemical reactions (Fig. S4). These findings indicate that on stagnation day, the limited dispersion caused by weak air flow plays a dominant role in the accumulation of surface ozone levels, while horizontal and vertical transport processes contribute to the localized enhancement of ozone concentrations. In contrast, recirculation day was primarily influenced by the vertical transport (VTRANS) process, which became the key driver of ozone concentration increases in the lower layers (1–2 layers).

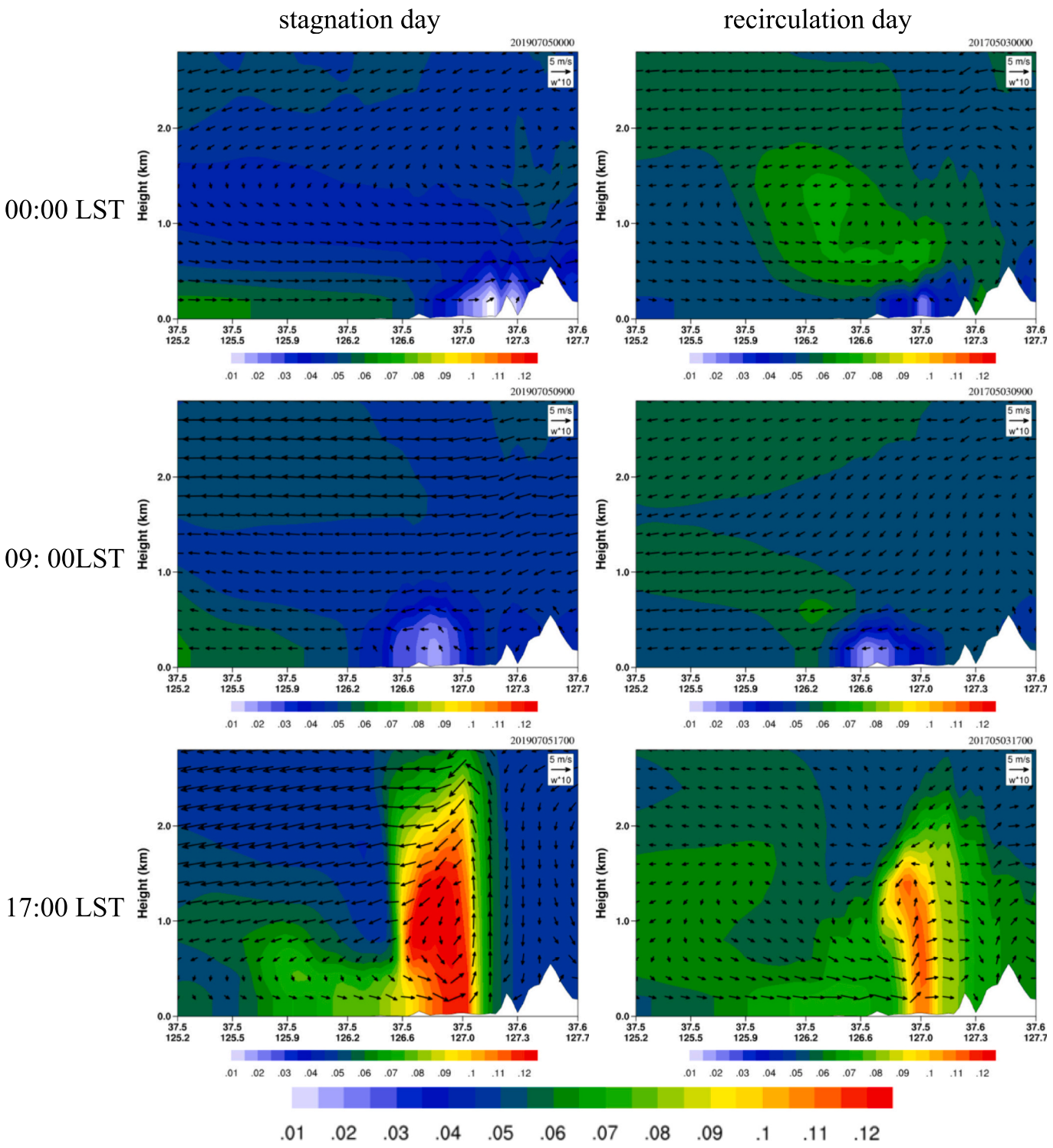

Fig. 9. Vertical cross-section (along the line A-B in Fig. 2) of the ozone (ppm) and wind vectors. The black line indicates the location of Seoul.

This was attributed to the vertical mixing of two sources of ozone: residual ozone present around 500 m altitude from the previous night and ozone produced in the upper layers through photochemical reactions during the daytime (Fig. S4). The IPR analysis for upwind areas of Seoul (near longitude 126.2°) revealed that residual ozone at approximately 500 m altitude was transported to Seoul via horizontal transport (Fig. S5). This transported residual ozone, when combined with photochemical production, contributed significantly to surface ozone levels through vertical mixing. On recirculation day, the VTRANS process accounted for an average increase of 0.02 ppm in surface ozone concentrations during daytime hours. Both stagnation and recirculation days exhibited the highest positive contributions from the photochemical (CHEM) process, underscoring the critical role of photochemical ozone production in increasing concentrations (Fig. S4). On stagnation day, ozone produced in the upper layers by photochemical reactions contributed 0.01 ppm to surface concentrations through VTRANS. On recirculation day, while the contribution from CHEM in the upper layers was comparatively lower, the VTRANS process showed a higher

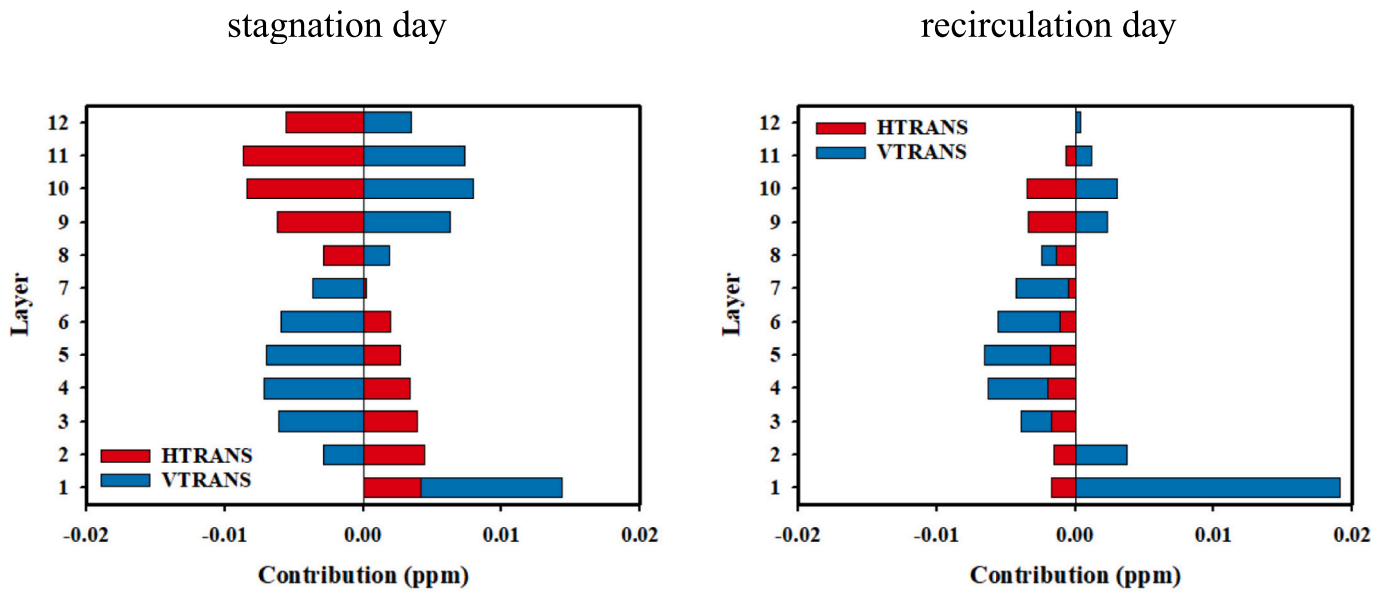

Fig. 10. Contribution of horizontal transport (HTRANS) and vertical transport (VTRANS) processes to ozone concentration over Seoul.

contribution of 0.02 ppm, reflecting the influence of residual ozone transported from the previous day.

These results highlight distinct differences in the mechanisms driving surface ozone increases between stagnation and recirculation days. On stagnation day, the accumulation of locally produced ozone, combined with limited regional transport, was the dominant factor. In contrast, on recirculation day, the transport and vertical mixing of residual ozone from the previous day played a more substantial role. The influence of the sea breeze on recirculation day facilitated the inland transport of residual ozone, which contributed to the increase in surface ozone concentrations in Seoul. In summary, the comparative analysis of stagnation and recirculation days underscores the importance of understanding the combined effects of local meteorology, transport processes, and residual ozone dynamics in explaining high surface ozone episodes in urban areas like Seoul.

4. Summary and conclusion

In this study, we employed methods based on previous research to classify local circulations in Seoul during the summer (May–August) from 2016 to 2021 into the Stagnation, Recirculation, and Ventilation types using wind observation data. The classification was achieved by calculating the recirculation factor (RF), defined as the ratio of the air's net displacement distance (L) to the actual displacement distance (S). Among these types, the Stagnation type was the most prevalent, accounting for approximately 34 % of the days. It was characterized by the highest daily maximum ozone concentrations and the weakest average wind speeds. Stagnation conditions also exhibited more extreme ozone concentration ranges, with unfavorable dispersion conditions (weak winds) contributing to the accumulation of ozone. At the same time, the rapid titration of ozone due to NOx emissions from local sources resulted in lower nighttime ozone concentrations. Conversely, the Recirculation type occurred on 16 % of the days and exhibited relatively lower daily maximum ozone concentrations compared to stagnation days. To further investigate the mechanisms driving high ozone concentrations under stagnation and recirculation conditions, representative case days for each type were selected based on meteorological and ozone observation data, supported by backward trajectory analysis using FLEXPART. Numerical simulations of meteorology and air quality were performed using the WRF and CMAQ models. While the horizontal distribution of ozone concentrations showed a typical diurnal pattern—with higher concentrations during the daytime due to active photochemical reactions and lower concentrations at night—the vertical distribution revealed distinct differences between the two types.

On recirculation day, elevated ozone concentrations (~0.07 ppm) were observed at altitudes above 500 m during the early morning. This suggests that ozone transported offshore by nighttime land breezes remained aloft over the sea and was subsequently transported back inland by the development of daytime sea breezes. Once transported inland, this ozone was vertically mixed from the upper layers to the surface in Seoul, contributing significantly to the increase in surface ozone concentrations. This transport and mixing mechanism was further validated by the IPR analysis, which highlighted the critical role of vertical transport in enhancing surface ozone levels on recirculation day. In contrast, on stagnation day, no significant ozone accumulation was observed over the sea during nighttime or early morning. This indicates that the extremely weak atmospheric flow inhibited the transport of pollutants offshore via the nighttime land breeze, resulting in their retention within the urban area.

This study enhances the understanding of how local circulations, specifically stagnation and recirculation, influence high ozone concentration episodes in Seoul. The findings indicate that on recirculation day, sea breezes transport pollutants inland, including residual ozone, which is subsequently mixed vertically to the surface. This process, combined with ozone production through photochemical reactions, significantly contributes to elevated surface ozone concentrations. Conversely, on stagnation day, limited dispersion due to weak air flow and the accumulation of ozone produced by photochemical reactions were the primary drivers of high ozone levels.

While the results highlight the critical role of local circulations, the occurrence and intensity of high ozone concentrations are influenced by additional factors such as synoptic-scale conditions, sea breeze strength, and proximity to the coastline. Thus, further climatological studies are needed to assess the variability and long-term impacts of recirculation-related sea breeze circulations. Additionally, this study focused on specific case days, and future research should explore whether the observed mechanisms and patterns are consistent across multiple events. Expanding the scope to include diverse meteorological conditions will be essential for validating and generalizing these findings, thereby improving our understanding of urban ozone dynamics.

CRediT authorship contribution statement

Jung-Woo Yoo: Writing – original draft, Visualization, Resources,

Investigation, Formal analysis, Data curation, Conceptualization. **Soon-Hwan Lee:** Writing – review & editing, Supervision, Project administration, Methodology, Funding acquisition.

Declaration of competing interest

The authors declare the following financial interests/personal relationships which may be considered as potential competing interests:

SOON-HWAN LEE reports financial support was provided by National Research Foundation of Korea. SOON-HWAN LEE reports financial support was provided by Ministry of Education. If there are other authors, they declare that they have no known competing financial interests or personal relationships that could have appeared to influence the work reported in this paper.

Acknowledgements

This research was supported by the Basic Science Research Program through the National Research Foundation of Korea (NRF), funded by the Ministry of Education (NRF-2020R1A6A1A03044834) and the Korean Government (MSIT) (No. 2022R1A2C1093229).

Appendix A. Supplementary data

Supplementary data to this article can be found online at https://doi.org/10.1016/j.atmosres.2025.107934.

Data availability

Data will be made available on request.

References

Abe, S., Yoshida, T., 1982. The effect of the width of a peninsula to the sea-breeze. J. Meteorol. Soc. Japan. Ser. II 60 (5), 1074–1084. https://doi.org/10.2151/jmsj1965.60.5_1074.

Allwine, K.J., Whiteman, C.D., 1994. Single-station integral measures of atmospheric stagnation, recirculation and ventilation. Atmos. Environ. 28 (4), 713–721.

An, J., Zou, J., Wang, J., Lin, X., Zhu, B., 2015. Differences in ozone photochemical characteristics between the megacity Nanjing and its suburban surroundings, Yangtze River Delta, China. Environ. Sci. Pollut. Res. 22, 19607–19617. https://doi.org/10.1007/s11356-015-5177-0.

Brioude, J., Arnold, D., Stohl, A., Cassiani, M., Morton, D., Seibert, P., Angevine, W., Evan, S., Dingwell, A., Fast, J.D., Easter, R.C., Pisso, I., Burkhart, J., Wotawa, G., 2013. The Lagrangian particle dispersion model FLEXPART-WRF version 3.1. Geosci. Model Dev. 6 (6), 1889–1904. https://doi.org/10.5194/gmd-6-1889-2013.

Byun, D., Schere, K.L., 2006. Review of the governing equations, computational algorithms, and other components of the models-3 Community Multiscale Air Quality (CMAQ) modeling system. Appl. Mech. Rev. 59 (2), 51–76. https://doi.org/10.1115/1.2128636.

Caicedo, V., Rappenglueck, B., Cuchiara, G., Flynn, J., Ferrare, R., Scarino, A.J., Berkoff, T., Senff, C., Langford, A., Lefer, B., 2019. Bay breeze and sea breeze circulation impacts on the planetary boundary layer and air quality from an observed and modeled DISCOVER-AQ Texas case study. J. Geophys. Res. Atmos. 124 (13), 7359–7378. https://doi.org/10.1029/2019JD030523.

Cariolle, D., Teyssèdre, H., 2007. A revised linear ozone photochemistry parameterization for use in transport and general circulation models: Multi-annual simulations. Atmos. Chem. Phys. 7 (9), 2183–2196. https://doi.org/10.5194/acp-7-2183-2007.

Colombi, N.K., Jacob, D.J., Yang, L.H., Zhai, S., Shah, V., Grange, S.K., Yantosca, R.M., Kim, S., Liao, H., 2023. Why is ozone in South Korea and the Seoul metropolitan area so high and increasing? Atmos. Chem. Phys. 23 (7), 4031–4044. https://doi.org/10.5194/acp-23-4031-2023.

Cuesta, J., Kanaya, Y., Takigawa, M., Dufour, G., Eremenko, M., Foret, G., Miyazaki, K., Beekmann, M., 2018. Transboundary ozone pollution across East Asia: daily evolution and photochemical production analysed by IASI + GOME2 multispectral satellite observations and models. Atmos. Chem. Phys. 18 (13), 9499–9525. https://doi.org/10.5194/acp-18-9499-2018.

Day, D.B., Xiang, J., Mo, J., Li, F., Chung, M., Gong, J., Weschler, C.J., Ohman-Strickland, P.A., Sundell, J., Weng, W., Zhang, Y., Zhang, J.J., 2017. Association of ozone exposure with cardiorespiratory pathophysiologic mechanisms in healthy adults. JAMA Intern. Med. 177 (9), 1344–1353. https://doi.org/10.1001/jamainternmed.2017.2842.

Dueñas, C., Fernández, M.C., Caete, S., Carretero, J., Liger, E., 2002. Assessment of ozone variations and meteorological effects in an urban area in the Mediterranean Coast. Sci. Total Environ. 299 (1–3), 97–113. https://doi.org/10.1016/S0048-9697(02)00251-6.

Emery, C.A., Tai, E., Yarwood, G., 2001. Enhanced meteorological modeling and performance evaluation for two Texas ozone episodes. In: Prepared for the Texas Natural Resource Conservation Commission. ENVIRON International Corporation, Novato, CA.

Freitas, E.D., Rozoff, C.M., Cotton, W.R., Silva Dias, P.L., 2007. Interactions of an urban heat island and sea-breeze circulations during winter over the metropolitan area of São Paulo, Brazil. Boundary-Layer Meteorol. 122, 43–65. https://doi.org/10.1007/s10546-006-9091-3.

Garrido-Perez, J.M., Ordóñez, C., García-Herrera, R., Barriopedro, D., 2018. Air stagnation in Europe: Spatiotemporal variability and impact on air quality. Sci. Total Environ. 645, 1238–1252. https://doi.org/10.1016/j.scitotenv.2018.07.238.

Ghim, Y.S., Chang, Y.S., 2000. Characteristics of ground-level ozone distributions in Korea for the period of 1990-1995. J. Geophys. Res. 105 (D7), 8877–8890. https://doi.org/10.1029/1999JD901179.

Gipson, G.L., 1999. Process analysis. In: Byun, D.W., Ching, J.K.S. (Eds.), Science Algorithms of the EPA Models-3 Community Multiscale Air Quality (CMAQ) Modeling System. US Environ. Prot. Agency, Washington DC, USA 16-1–16-20. EPA/600/R-99/030 (NTIS PB2000-100561).

Grulke, N.E., Heath, R.L., 2020. Ozone effects on plants in natural ecosystems. Plant Biol. 22, 12–37. https://doi.org/10.1111/plb.12971.

Han, H., Liu, J., Shu, L., Wang, T., Yuan, H., 2020. Local and synoptic meteorological influences on daily variability in summertime surface ozone in eastern China. Atmos. Chem. Phys. 20 (1), 203–222. https://doi.org/10.5194/acp-20-203-2020.

He, C., Lu, X., Wang, Haolin, Wang, Haichao, Li, Y., He, G., He, Y., Wang, Y., Zhang, Y., Liu, Y., Fan, Q., Fan, S., 2022. The unexpected high frequency of nocturnal surface ozone enhancement events over China: Characteristics and mechanisms. Atmos. Chem. Phys. 22 (23), 15243–15261. https://doi.org/10.5194/acp-22-15243-2022.

Hollaway, M.J., Arnold, S.R., Challinor, A.J., Emberson, L.D., 2012. Intercontinental trans-boundary contributions to ozone-induced crop yield losses in the Northern Hemisphere. Biogeosciences 9 (1), 271–292. https://doi.org/10.5194/bg-9-271-2012.

Hu, X.M., Doughty, D.C., Sanchez, K.J., Joseph, E., Fuentes, J.D., 2012. Ozone variability in the atmospheric boundary layer in Maryland and its implications for vertical transport model. Atmos. Environ. 46, 354–364. https://doi.org/10.1016/j.atmosenv.2011.09.054.

Hu, J., Li, Y., Zhao, T., Liu, J., Hu, X.M., Liu, D., Jiang, Y., Xu, J., Chang, L., 2018. An important mechanism of regional O_3 transport for summer smog over the Yangtze River Delta in eastern China. Atmos. Chem. Phys. 18 (22), 16239–16251. https://doi.org/10.5194/acp-18-16239-2018.

Jacob, D.J., Winner, D.A., 2009. Effect of climate change on air quality. Atmos. Environ. 43 (1), 51–63. https://doi.org/10.1016/j.atmosenv.2008.09.051.

Kim, H.C., Lee, D., Ngan, F., Kim, B.U., Kim, S., Bae, C., Yoon, J.H., 2021. Synoptic weather and surface ozone concentration in South Korea. Atmos. Environ. 244, 117985. https://doi.org/10.1016/j.atmosenv.2020.117985.

Lee, S.H., Park, G.Y., Chang, L.S., Song, C.K., 2015. Behavior of air particles associated with atmospheric recirculation over complex coastal area. Asia-Pacific J. Atmos. Sci. 51, 311–322. https://doi.org/10.1007/s13143-015-0080-7.

Levy, I., Dayan, U., Mahrer, Y., 2008. A five-year study of coastal recirculation and its effect on air pollutants over the East Mediterranean region. J. Geophys. Res. Atmos. 113 (D16). https://doi.org/10.1029/2007JD009529.

Levy, I., Dayan, U., Mahrer, Y., 2010. Differing atmospheric scales of motion and their impact on air pollutants. Int. J. Climatol. 30 (4), 612–619. https://doi.org/10.1002/joc.1905.

Li, S., Wang, T., Huang, X., Pu, X., Li, M., Chen, P., Yang, X.Q., Wang, M., 2018. Impact of East Asian summer monsoon on surface ozone pattern in China. J. Geophys. Res. Atmos. 123 (2), 1401–1411. https://doi.org/10.1002/2017JD027190.

Li, W., Wang, Y., Bernier, C., Estes, M., 2020. Identification of sea breeze recirculation and its effects on ozone in Houston, TX, during DISCOVER-AQ 2013. J. Geophys. Res. Atmos. 125 (22), 1–21. https://doi.org/10.1029/2020JD033165.

Liu, C., He, C., Wang, Y., He, G., Liu, N., Miao, S., Wang, H., Lu, X., Fan, S., 2023. Characteristics and mechanism of a persistent ozone pollution event in Pearl River Delta induced by typhoon and subtropical high. Atmos. Environ. 310, 119964. https://doi.org/10.1016/j.atmosenv.2023.119964.

Loughner, C.P., Tzortziou, M., Follette-Cook, M., Pickering, K.E., Goldberg, D., Satam, C., Weinheimer, A., Crawford, J.H., Knapp, D.J., Montzka, D.D., Diskin, G.S., Dickerson, R.R., 2014. Impact of bay-breeze circulations on surface air quality and boundary layer export. J. Appl. Meteorol. Climatol. 53 (7), 1697–1713. https://doi.org/10.1175/JAMC-D-13-0323.1.

Martins, D.K., Stauffer, R.M., Thompson, A.M., Knepp, T.N., Pippin, M., 2012. Surface ozone at a coastal suburban site in 2009 and 2010: Relationships to chemical and meteorological processes. J. Geophys. Res. Atmos. 117 (D5), 1–16. https://doi.org/10.1029/2011JD016828.

Mirowsky, J.E., Carraway, M.S., Dhingra, R., Tong, H., Neas, L., Diaz-Sanchez, D., Cascio, W., Case, M., Crooks, J., Hauser, E.R., Elaine Dowdy, Z., Kraus, W.E., Devlin, R.B., 2017. Ozone exposure is associated with acute changes in inflammation, fibrinolysis, and endothelial cell function in coronary artery disease patients. Environ. Health 16, 1–10. https://doi.org/10.1186/s12940-017-0335-0.

Miyazaki, K., Sekiya, T., Fu, D., Bowman, K.W., Kulawik, S.S., Sudo, K., Walker, T., Kanaya, Y., Takigawa, M., Ogochi, K., Eskes, H., Boersma, K.F., Thompson, A.M., Gaubert, B., Barre, J., Emmons, L.K., 2019. Balance of emission and dynamical controls on ozone during the Korea-United States air quality campaign from multiconstituent satellite data assimilation. J. Geophys. Res. Atmos. 124 (1), 387–413. https://doi.org/10.1029/2018JD028912.

Monteiro, A., Strunk, A., Carvalho, A., Tchepel, O., Miranda, A.I., Borrego, C., Saavedra, S., Rodríguez, A., Souto, J., Casares, J., Friese, E., Elbern, H., 2012. Investigating a high ozone episode in a rural mountain site. Environ. Pollut. 162, 176–189. https://doi.org/10.1016/j.envpol.2011.11.008.

Nauth, D., Loughner, C.P., Tzortziou, M., 2023. The influence of synoptic-scale wind patterns on column-integrated nitrogen dioxide, ground-level ozone, and the development of sea-breeze circulations in the New York city metropolitan area. J. Appl. Meteorol. Climatol. 62 (6), 645–655. https://doi.org/10.1175/JAMC-D-22-0145.1.

Russo, A., Gouveia, C., Levy, I., Dayan, U., Jerez, S., Mendes, M., Trigo, R., 2016. Coastal recirculation potential affecting air pollutants in Portugal: the role of circulation weather types. Atmos. Environ. 135, 9–19. https://doi.org/10.1016/j.atmosenv.2016.03.039.

Russo, A., Gouveia, C.M., Soares, P.M.M., Cardoso, R.M., Mendes, M.T., Trigo, R.M., 2018. The unprecedented 2014 Legionnaires' disease outbreak in Portugal: atmospheric driving mechanisms. Int. J. Biometeorol. 62, 1167–1179. https://doi.org/10.1007/s00484-018-1520-8.

Seo, J., Youn, D., Kim, J.Y., Lee, H., 2014. Extensive spatiotemporal analyses of surface ozone and related meteorological variables in South Korea for the period 1999-2010. Atmos. Chem. Phys. 14 (12), 6395–6415. https://doi.org/10.5194/acp-14-6395-2014.

Seo, S., Kim, S.W., Kim, K.M., Lamsal, L.N., Jin, H., 2021. Reductions in NO_2 concentrations in Seoul, South Korea detected from space and ground-based monitors prior to and during the covid-19 pandemic. Environ. Res. Commun. 3 (5). https://doi.org/10.1088/2515-7620/abed92.

Shin, D., Song, S., Ryoo, S.B., Lee, S.S., 2020. Variations in ozone concentration over the mid-latitude region revealed by ozonesonde observations in Pohang, South Korea. Atmosphere 11 (7). https://doi.org/10.3390/atmos11070746.

Sillman, S., 1999. The relation between ozone, NOx and hydrocarbons in urban and polluted rural environments. Atmos. Environ. 33 (12), 1821–1845. https://doi.org/10.1016/S1474-8177(02)80015-8.

Silva, R.A., West, J.J., Zhang, Y., Anenberg, S.C., Lamarque, J.F., Shindell, D.T., Collins, W.J., Dalsoren, S., Faluvegi, G., Folberth, G., Horowitz, L.W., Nagashima, T., Naik, V., Rumbold, S., Skeie, R., Sudo, K., Takemura, T., Bergmann, D., Cameron-Smith, P., Cionni, I., Doherty, R.M., Eyring, V., Josse, B., Mackenzie, I.A., Plummer, D., Righi, M., Stevenson, D.S., Strode, S., Szopa, S., Zeng, G., 2013. Global premature mortality due to anthropogenic outdoor air pollution and the contribution of past climate change. Environ. Res. Lett. 8 (3). https://doi.org/10.1088/1748-9326/8/3/034005.

Skamarock, W.C., Klemp, J.B., Dudhia, J., Gill, D.O., Barker, D.M., Duda, M.G., Huang, X. Y., Wang, W., Powers, J.G., 2008. A Description of the Advanced Research WRF Version 3. NCAR technical note, NCAR/TN-475+aSTR.

Wang, T., Du, H., Zhao, Z., Russo, A., Zhang, J., Zhou, C., 2022. The impact of potential recirculation on the air quality of Bohai Bay in China. Atmos. Pollut. Res. 13 (1), 101268. https://doi.org/10.1016/j.apr.2021.101268.

Wu, Y.L., Lin, C.H., Lai, C.H., Lai, H.C., Young, C.Y., 2010. Effects of local circulations, turbulent internal boundary layers, and elevated industrial plumes on coastal ozone pollution in the downwind Kaohsiung urban–industrial complex. Terr. Atmos. Ocean. Sci. 21 (2), 343–357. https://doi.org/10.3319/TAO.2009.04.14.01(A).

Yeo, M.J., Kim, Y.P., 2021. Long-term trends of surface ozone in Korea. J. Clean. Prod. 294, 125352. https://doi.org/10.1016/j.jclepro.2020.125352.

Yoo, J.W., Park, S.Y., Lee, K., Lee, D., Lee, Y., Lee, S.H., 2022. Impacts of plateau-induced lee troughs on regional $PM_{2.5}$ over the Korean Peninsula. Atmos. Pollut. Res. 13 (7), 101459. https://doi.org/10.1016/j.apr.2022.101459.

Yoo, J.W., Park, S.Y., Jo, H.Y., Jeong, Y., Lee, H.J., Kim, Cheol-Hee, Lee, S.H., 2024a. Assessing the role of cold front passage and synoptic patterns on air pollution in the Korean Peninsula. Environ. Pollut. 348, 123803. https://doi.org/10.1016/j.envpol.2024.123803.

Yoo, J.W., Park, S.Y., Jeon, W., Jung, J., Park, J., Mun, J., Kim, D., Lee, S.H., 2024b. Understanding the physical mechanisms of $PM_{2.5}$ formation in Seoul, Korea: assessing the role of aerosol direct effects using the WRF-CMAQ model. Air Qual. Atmos. Health 1–14. https://doi.org/10.1007/s11869-024-01538-x.

Zhang, J., Chen, Q., Wang, Q., Ding, Z., Sun, H., Xu, Y., 2019. The acute health effects of ozone and $PM_{2.5}$ on daily cardiovascular disease mortality: a multi-center time series study in China. Ecotoxicol. Environ. Saf. 174, 218–223. https://doi.org/10.1016/j.ecoenv.2019.02.085.

Zhang, Y., Zhao, T., Sun, X., Bai, Y., Shu, Z., Fu, W., Lu, Z., Wang, X., 2024. Ozone pollution aggravated by mountain-valley breeze over the western Sichuan Basin, Southwest China. Chemosphere 361, 142445. https://doi.org/10.1016/j.chemosphere.2024.142445.